HHS Public Access

Author manuscript

Cell Rep. Author manuscript; available in PMC 2016 November 17.

Published in final edited form as:

Cell Rep. 2015 November 17; 13(7): 1481–1492. doi:10.1016/j.celrep.2015.10.018.

An Antifungal Combination Matrix Identifies a Rich Pool of Adjuvant Molecules that Enhance Drug Activity Against Diverse Fungal Pathogens

Nicole Robbins[1], **Michaela Spitzer**[1], **Tennison Yu**[1], **Robert P. Cerone**[2], **Anna K. Averette**[5], **Yong-Sun Bahn**[6], **Joseph Heitman**[5], **Donald C. Sheppard**[3], **Mike Tyers**[4], and **Gerard D. Wright**[1,*]

[1]Michael G. DeGroote Institute for Infectious Disease Research and the Department of Biochemistry and Biomedical Sciences, McMaster University, Hamilton, Ontario, L8N 3Z5, Canada

[2]Department of Microbiology and Immunology, McGill University, Montréal, Québec, H3G 1A4, Canada

[3]Department of Medicine, McGill University, Montréal, Québec, H3G 1A4, Canada

[4]Institute for Research in Immunology and Cancer, Université de Montréal, Pavillon Montréal, Québec, H3C 3J7, Canada

[5]Departments of Molecular Genetics and Microbiology, Medicine, and Pharmacology and Cancer Biology, Duke University Medical Center, Durham, North Carolina, 27710, USA

[6]Department of Biotechnology, College of Life Science and Biotechnology, Yonsei University, Seoul, 120-749, Republic of Korea

SUMMARY

There is an urgent need to identify new treatments for fungal infections. By combining sub-lethal concentrations of the known antifungals fluconazole, caspofungin, amphotericin B, terbinafine, benomyl and cyprodinil with ~3600 compounds in diverse fungal species, we generated a deep reservoir of chemical-chemical interactions termed the Antifungal Combinations Matrix (ACM). Follow-up susceptibility testing against a fluconazole resistant isolate of *C. albicans* unveiled ACM combinations capable of potentiating fluconazole in this clinical strain. We used chemical genetics to elucidate the mode-of-action of the antimycobacterial drug clofazimine, a compound with unreported antifungal activity that synergized with several antifungals. Clofazimine induces a

[*]**Corresponding Author:** Gerard D. Wright, Michael G. DeGroote Institute for Infectious Disease Research and the Department of Biochemistry and Biomedical Sciences, McMaster University, Hamilton, Ontario, Canada, L8N 3Z5. Tel.: +1 905 525 9140/ext. 20230, Fax: +1 905 528 5330, wrightge@mcmaster.ca.

AUTHOR CONTRIBUTIONS Conceptualization, N.R., M.T., and G.D.W.; Methodology, N.R., Y.S.B., J.H., D.C.S, and G.D.W.; Formal Analysis, N.R., M.S., Investigation, N.R., T.Y., R.P.C., A.K.A., and Y.S.B.; Writing – Original Draft, N.R and G.D.W.; Writing – Review & Editing, N.R., M.S., J.H., D.C.S., M.T., and G.D.W.; Visualization, N.R., M.S.; Funding Acquisition, M.T and G.D.W.; Resources, J.H.; Supervision, J.H., D.C.S., M.T., and G.D.W.

cell membrane stress for which the Pkc1 signaling pathway is required for tolerance. Further tests against additional fungal pathogens, including *Aspergillus fumigatus*, highlighted that clofazimine exhibits efficacy as a combination agent against multiple fungi. Thus, the ACM is a rich reservoir of chemical combinations with therapeutic potential against diverse fungal pathogens.

INTRODUCTION

Fungal pathogens have emerged as a leading cause of human mortality. Current estimates suggest death due to invasive fungal infections is on par with more well known infectious diseases such as tuberculosis (Brown et al., 2012; Denning and Bromley, 2015), with costs to the health care system of ~$2.6 billion annually in the United States alone (Wilson et al., 2002). These staggering clinical and economic impacts are in large part due to the limited number of validated cellular targets available in fungi to exploit for drug discovery, and the ability of fungal pathogens to thwart therapeutic regimens by evolving resistance to current treatments. *Candida albicans*, *Cryptococcus neoformans*, and *Aspergillus fumigatus* represent the most prevalent fungal pathogens of humans (Brown et al., 2012). Each of these species is responsible for hundreds of thousands of infections annually with unacceptably high mortality rates due to poor diagnostics and limited treatment options (Brown et al., 2012). Furthermore, the rapid emergence of drug resistance in *Candida* species poses a serious threat to human health as identified by the Centre for Disease Control and Prevention (CDC, 2013). The challenge that remains in the medical mycology community is the identification of therapies with efficacy against fungal pathogens while maintaining minimal human toxicity.

Due to the evolutionary conservation of eukaryotic gene function from fungi to humans, only a limited number of antifungal drugs exhibit selective toxicity to fungi. The polyenes, which cause severe nephrotoxicity, form large extramembranous aggregates that extract the essential membrane-lipid ergosterol from the plasma membrane (Anderson et al., 2014). The azoles inhibit ergosterol biosynthesis and impede cellular growth, but because these compounds are merely fungistatic resistance is readily acquired. The only new class of antifungal to reach the clinic in decades is the echinocandins, which inhibit synthesis of β-(1,3) glucan, a key component of the fungal cell wall (Ostrosky-Zeichner et al., 2010). This paucity of fungal-specific targets is problematic given the prevalence of cross-resistance to all drugs with a common target, and indeed resistance to all widely deployed antifungals has been documented in both the laboratory and the clinic (Shapiro et al., 2011).

Despite efforts over the past several decades to discover novel treatments for fungal infections, there remains a paucity of new drug leads and new drug targets. Recent efforts to understand the complex networks that underpin the biology of fungi in model species suggest new therapeutic strategies. Large-scale genetic and proteomic studies in the budding yeast *Saccharomyces cerevisiae* have revealed that cellular behavior is controlled by a highly interconnected and functionally redundant network of gene and protein interactions (Costanzo et al., 2010; Sharom et al., 2004). While only ~1000 of the ~6000 genes in *S. cerevisiae* are essential for growth, systematic efforts to simultaneously disrupt any two non-essential genes in the same cell has revealed over 170,000 synthetic lethal combinations

(Costanzo et al., 2010). This redundancy, referred to as genetic buffering, in part explains the difficulty of identifying single compounds that result in cellular toxicity. The vast network of synthetic lethal genetic interactions represents an untapped target space for drug discovery, as in principle, combinations of compounds that perturb fungal genetic networks at two or more nodes may result in selective toxicity. Furthermore, combinatorial inhibition can confer enhanced efficacy and specificity compared to individual drug treatments, and can slow the evolution of resistance (Zimmermann et al., 2007). Ad hoc drug combinations discovered by trial and error have been widely used against many diseases. For example, the current gold standard antifungal regimen for cryptococcal meningitis is a combination of amphotericin B and 5-flucytosine (Day et al., 2013). The systematic discovery of active drug combinations to treat fungal infections, predicated on the concept of extensive genetic network redundancy, is a potentially rich source of new antifungal agents.

The re-purposing of previously approved drugs for new indications has emerged as one means to expedite drug development because the known toxicology and pharmacology lowers regulatory barriers and cost. The combination of established antifungals with re-purposed drugs from other indications holds considerable promise. In an early example, calcineurin or target of rapamycin (TOR) inhibitors improved the efficacy of fluconazole against a variety of pathogenic fungi (Blankenship et al., 2003). More recently, the Hsp90 inhibitor 17-AAG was found to synergize with fluconazole against *C. albicans* in a *Galleria mellonella* model of systemic candidiasis, and in a rat catheter model of biofilm infection (Cowen et al., 2009; Robbins et al., 2011). A large-scale systematic analysis of chemical-chemical interactions identified 148 bioactive molecules that potentiate the activity of fluconazole towards diverse fungal species, including clinical pathogens (Spitzer et al., 2011). Another screen of off-patent drugs revealed 15 compounds with activity against *C. neoformans* (Butts et al., 2013). High-throughput screens for synergistic enhancers of known antifungal agents thus have the potential to yield effective combination therapeutics against clinically relevant pathogens.

In this study, we screened sub-lethal concentrations of six known antifungals in combination with ~3600 different bioactive compounds to uncover synergistic drug combinations. Parallel screens were performed in the model yeasts *S. cerevisiae* and *Schizosaccharomyces pombe*, as well as in the fungal pathogens *C. albicans* and *C. neoformans* to generate the most comprehensive analysis of drug combinations in fungi to date. This dataset of drug interactions, which we have termed the Antifungal Combination Matrix (ACM), contains hundreds of chemical combinations that abrogate fungal growth, often in an antifungal- and species-specific manner. We show that a number of antifungal combinations are active towards an isolate of *C. albicans* that had acquired fluconazole resistance in the clinic. Chemical-genetic profiling of clofazimine, an antimycobacterial agent for which antifungal activity has not been described, suggested that it induces a Pkc1-dependent cell membrane stress response. We further show that clofazimine is a general potentiator of antifungal activity in fungal species separated by ~1 billion years of evolution. Thus, the ACM represents a unique resource of chemical probes for the study of fungal biology, and an entry point for discovery of combination therapeutics against diverse fungal pathogens.

RESULTS

The Antifungal Combination Matrix

To identify molecules that potentiate known antifungal agents, we selected six entry point drugs. We chose four clinically relevant drugs with well-characterized targets: amphotericin B (ergosterol, cell membrane), fluconazole (Erg11; ergosterol biosynthesis), terbinafine (Erg1; ergosterol biosynthesis) and caspofungin (β-glucan synthase, cell wall synthesis). We also selected two agricultural fungicides: benomyl, a microtubule inhibitor, and cyprodinil, a compound whose mode of action remains enigmatic. High-throughput combination screens were performed against four different fungal species: *S. cerevisiae*, *S. pombe*, *C. albicans* and *C. neoformans*. These evolutionarily divergent genera were chosen in order to identify combination agents in model yeast species where mode of action can be readily probed using advanced functional genomic reagents, and in clinically relevant fungal pathogens. Each species was screened using compounds from the McMaster Bioactives collection, a library of ~3600 unique small molecules derived from commercial sources. All of the screens were performed with 12.5 μM of compound in the absence and presence of ¼ Minimum Inhibitory Concentration (MIC) of the antifungal drug (Table S1). This concentration regime enabled identification of antifungal potentiators that had minimal growth effects on their own. Residual activity was calculated for each compound and data were normalized for plate- and row/column specific effects as described previously (Table S2) (Spitzer et al., 2011). Compounds that were greater than three median absolute deviations (MADs) below the diagonal, had less than 50% reduction of growth on their own, and resulted in greater than 80% growth inhibition in the presence of antifungal, were chosen for further analysis (Figure S1). This data set called the Antifungal Combination Matrix (ACM), contained over 228,000 data points for ~86,000 unique pairwise chemical-chemical interactions, and identified 1550 drug combinations that showed efficacy against at least one fungal species (Figure 1 and Table S3). The ACM represents the largest high-throughput screening effort for combination agents against model yeasts and pathogenic fungi.

To evaluate how the 1550 active compounds identified in the ACM are related to one another, we displayed the hits as a comprehensive network of chemical-chemical interactions that connect each antifungal entry point drug to the chemicals that were screened as a function of the species in which the interaction was identified (Figure 1). This unveiled an intricate pattern of chemical-chemical combinations capable of abrogating fungal growth. Different screens had dramatically different numbers of compounds that increased the efficacy of each antifungal agent, with hit rates as high as 7.4% for the amphotericin B screen performed in *C. neoformans* and as low as 0.18% for the benomyl screen performed in *C. neoformans* (Figure 1). These hit rates were within the range reported from other drug combination screens (Borisy et al., 2003; Spitzer et al., 2011). More potentiators were identified with the antifungals caspofungin and amphotericin B, which disrupt cell wall or membrane (Figure 1). Benomyl, cyprodinil, fluconazole and terbinafine had markedly fewer hits that were more drug specific (Figure 1 and Figure S2), demonstrating different antifungal classes elicit dramatically different rates of potentiation with other small molecules.

The vast majority of the hits in the ACM were species- and/or antifungal specific, with only 22 compounds identified in more than five screens. We visualized all compounds in a heat map to reveal the specific conditions linked by these `high-connectivity' compounds (Figure 2). Small molecules that were identified most frequently as potentiators included tomatidine and chlorhexidine, identified in 13 and 12 screens respectively. Notably, both of these molecules are reported membrane perturbing agents (Gilbert and Moore, 2005; Simons et al., 2006). Separate chemical-species interaction networks for each antifungal drug revealed species-specific effects elicited by a majority of the combination treatments explored (Figure S2). For example, molecules that increased the efficacy of fluconazole, terbinafine, benomyl, and cyprodinil, were largely antifungal specific with little overlap across the different fungal species (Figure S2). In contrast, when examining potentiators of amphotericin B, *C. neoformans* and *C. albicans* shared the largest number of hits whereas *C. albicans* and *S. cerevisiae* shared a high number of caspofungin potentiators (Figure S2). In addition, *C. albicans* and *S. cerevisiae* both had a high number of compounds that increased the efficacy of both amphotericin B and caspofungin (Figure 1). Overall, the ACM represents an extensive resource of bioactive chemical space for antifungal drug discovery.

Hit validation and characterization

To explore a subset of the 1550 hits from the ACM, we chose eight compounds for additional drug susceptibility analysis. These eight compounds were chosen based on diversity of chemical class (Figure 3A), therapeutic use when known, and the screens in which they were identified (Table S4). We tested these eight compounds using standard concentration matrix (checkerboard) assays in combination with the clinically relevant antifungals caspofungin or fluconazole (Figure S3). Data were quantified by calculation of the fractional inhibitory concentration index (FICI), an accepted method for evaluating chemical interactions in infectious disease (Figure 3B) (Odds, 2003). Drug interactions are synergistic if the calculated FICI is below of 0.5, additive if the FICI is 0.5–0.99 and an FICI between 1.0–4.0 indicates no chemical-chemical interaction (Odds, 2003). Amiodarone hydrochloride, asiatic acid, clofazimine and cyclosporin A were synergistic with caspofungin against *C. albicans* and *S. cerevisiae* (Figure 3B and Table S5). Cyclosporin A was also synergistic with caspofungin against *S. pombe*, and clofazimine was synergistic with caspofungin against *C. neoformans* (Figure 3B and Table S5). Checkerboard assays performed with fluconazole revealed tomatidine as a potent synergizer of fluconazole against *C. albicans*, *S. cerevisiae*, and *C. neoformans* (Figure 3B and Table S5). Similarly, clofazimine was synergistic with fluconazole against *S. cerevisiae* and *C. neoformans*. All remaining drug interactions were either additive of showed no interaction (Table S5). In total 72 checkerboard assays were conducted with drug combinations from the primary screen. All hits from the screens were confirmed except for thapsigargin with fluconazole against *S. cerevisiae* (Figure S3, Figure S5 and Table S4). Overall, these detailed analyses verified interactions identified in the ACM.

A limitation of the azoles is that resistance readily evolves due to the fungistatic nature of the drug (Shapiro et al., 2011). To determine if any compounds rendered fluconazole fungicidal, we used tandem assays with an antifungal susceptibility test followed by spotting onto rich medium without inhibitors. We tested cidality for compounds that reduced growth

in the presence of fluconazole more so than growth in either drug individually (Figure S3). An overwhelming majority of the chemical-chemical interactions evaluated transformed fluconazole to a fungicidal drug (Figure 3B). These results suggest that the fluconazole enhancers may help suppress the emergence of antifungal resistance.

Drug combinations with efficacy against a *C. albicans* clinical isolate

In clinical settings, many thousands of antifungal resistant infections are diagnosed every year, particularly fluconazole-resistant *C. albicans* (CDC, 2013). Therefore, we evaluated the activity of fluconazole enhancers originally identified in the ACM against a bona fide fluconazole-resistant clinical isolate of *C. albicans*. This strain had a fluconazole MIC of 128 μg/mL, ~250-fold higher than the laboratory strain likely due to mutations identified in the azole target *ERG11* ($Erg11^{R264K}$), as well as in *TAC1* ($Tac1^{T225A}$), a transcriptional activator of ABC transporters. Of the 18 molecules tested, three increased the susceptibility of the resistant clinical isolate to fluconazole: chlorhexidine, tomatidine, and hypocrellin A (Figure 4A). In order to assess the robustness of these drug interactions, checkerboard assays were conducted and the FICI was used to evaluate synergy. All three molecules were highly synergistic with fluconazole with FICI values below 0.5 (Figure 4B), unveiling drug combinations with potent activity against a clinically relevant strain of *C. albicans*. Thus, a fraction of antifungal combinations with activity against a wild type strain of *C. albicans* are able to inhibit the growth of a fluconazole-resistant clinical isolate.

Mechanism of action of clofazimine

Clofazimine is currently used as an antimycobacterial agent but in our study showed broad-spectrum activity in combination with fluconazole and caspofungin. As clofazimine has not been described as an antifungal, we interrogated the mechanism of action using established genomic profiling methods (Giaever et al., 2004; Pierce et al., 2006). We profiled compound action in haploinsufficiency profiling (HIP) screens, in which the ~1000 diploid deletion strains heterozygous for essential genes were tested for drug sensitivity to identify candidate compound targets. Genes that encode the target of a compound are expected to be hypersensitive to that compound, as indicated by decreased fitness as measured by competitive growth (Giaever et al., 2004; Pierce et al., 2006). We validated our implementation of this methodology by re-identifying *ERG11* as the established target for fluconazole (Figure S4). The HIP profile generated for clofazimine was distinct from that observed with fluconazole in that a single gene was not markedly more sensitive to clofazimine relative to other genes in the pool. Among the heterozygous mutants most sensitive to clofazimine was *NEO1*, which encodes an essential aminophospholipid translocase required for membrane trafficking and vacuolar biogenesis (Table S6). *NEO1* haploinsufficiency is induced by cationic amphiphilic drugs (CADs) (Lee et al., 2014), a structural feature shared by clofazimine.

We profiled clofazimine action in homozygous deletion profiling (HOP) screens, in which the ~5000 deletion strains for non-essential genes were tested for drug sensitivity to identify chemical-genetic interactions indirectly associated with the compound target (Giaever et al., 2004; Pierce et al., 2006). Several gene deletion strains were sensitive to clofazimine including genes important for phospholipid transport, membrane organization, vesicle-

mediated transport, and localization (Figure 5), processes associated with membrane integrity and function (Lee et al., 2014). Moreover, the chemical-genetic profile observed with clofazimine is markedly similar to the structurally related membrane perturbing agent chlorpromazine (De Filippi et al., 2007). In addition, deletion of the copper-related genes *SOD1*, *CCS1*, and *CTR1* rendered cells sensitive to clofazimine (Figure 5), a feature shared by compounds that elicit high degrees of oxidative stress such as menadione (Lee et al., 2014). Clofazimine sensitivity of the top haploid deletion strains identified in our HOP analysis was confirmed using growth curve analysis (Figure S4). Based on our chemogenomic profile, we postulate that clofazimine may be exerting its effects by disrupting cellular membranes and/or through the generation of reactive oxygen species.

Clofazimine induces a cell membrane stress response and activates Pkc1

Our chemical-genetic profile implicated a dual mechanism of action for clofazimine. First, we tested our hypothesis that clofazimine elicits a cell membrane stress response. Chlorpromazine and clofazimine are both CADs consisting of a hydrophobic tricyclic ring and a hydrophilic side chain (Figure 6A). The hydrophobic moiety of chlorpromazine allows it to intercalate into the hydrocarbon phase of the membrane bilayer (De Filippi et al., 2007). At physiological pH, the tertiary dimethylpropylamine is protonated and engages in electrostatic interactions with cytosolic anionic lipids (Levin, 2005). Altering *in vitro* conditions by decreasing the pH of culture medium renders chlorpromazine in its protonated state prior to diffusion across the *S. cerevisiae* membrane, blocking cellular entry and impeding its toxic effects (De Filippi et al., 2007). We tested whether similar effects were observed with clofazimine by spotting wild type *S. cerevisiae* and a *rim101* mutant, which is hypersensitive to clofazimine, onto agar buffered at pH 5.5 or pH 8. At pH 5.5 cells were resistant to the effects of clofazimine (Figure 6B), presumably due to electrostatic interactions with the cellular membrane that blocked compound entry. At a more basic pH, clofazimine entered the cell and inhibited growth, particularly in the *rim101* mutant (Figure 6B). This suggests clofazimine interacts with the cellular membrane in a similar manner to chlorpromazine.

Drug-induced phospholipidosis (DIPL) is a phospholipid storage disorder associated with CADs. In yeast, DIPL arises from the selective buildup of CADs in the acidic vacuole, however loss of acidification reduces intracellular drug accumulation and mitigates toxicity (Anderson and Borlak, 2006). Inhibition of yeast vacuolar adenosine triphosphatase by bafilomycin A alleviated the fitness defect induced by clofazimine ($P < 0.01$, ANOVA, Bonferroni's Multiple Comparison Test, Figure 6C), in a similar manner to other CADs (Lee et al., 2014), supporting our hypothesis that clofazimine exerts its toxic effects through non-specific membrane perturbations. As high temperature increases turgor pressure and membrane stress on the cell (Levin, 2005), we predicted enhanced synergy between clofazimine and caspofungin at elevated temperature. Growth of both *S. cerevisiae* and *C. albicans* at 39°C exacerbated the synergy observed between caspofungin and clofazimine (Figure 6D). Perturbation of the cell membrane and/or cell wall can often be rescued by osmotic stabilization. In both *S. cerevisiae* and *C. albicans* the addition of the osmotic stabilizer sorbitol abrogated synergy observed between caspofungin and clofazimine (Figure S5A), suggesting osmotic support reduces the effects of membrane stress caused by

clofazimine. Checkerboard assays with clofazimine and the membrane targeting antifungal amphotericin B or the ergosterol biosynthesis inhibitor terbinafine also unveiled enhanced efficacy of the drug combination in all four species tested (Figure S5B).

Cells that experience membrane stress activate the Pkc1 signaling pathway, as measured by phosphorylation of the terminal MAP kinase Slt2 (Levin, 2005). We treated *S. cerevisiae* with clofazimine and monitored Slt2 phosphorylation. Exposure to clofazimine increased phosphorylation of Slt2 relative to total levels (Figure 6E). The phosphorylation of Slt2 induced by clofazimine occurred regardless of whether caspofungin, another activator of Pkc1 signaling, was present. Pkc1 is an essential protein in *S. cerevisiae*, therefore we monitored the growth of the *PKC1* heterozygous deletion mutant, as well as growth of homozygous deletion mutants elsewhere in the pathway in order to determine whether this signaling cascade was required for tolerance to clofazimine. All mutants displayed increased sensitivity to clofazimine compared to a wild type control strain ($P < 0.001$, ANOVA, Bonferroni's Multiple Comparison Test, Figure 6F), except for deletion of *SWI4*. We also tested a *pkc1*Δ/*pkc1*Δ homozygous deletion strain in *C. albicans*, where Pkc1 is not essential but is required for tolerance to cell membrane stress (LaFayette et al., 2010). Deletion of *PKC1* abolished growth of *C. albicans* in the presence of clofazimine and complementation of the *pkc1* mutation in a *pkc1/pkc1 + PKC1* strain restored growth back to wild type levels ($P < 0.001$, Figure 6F). Taken together, these data suggest that clofazimine elicits a cell membrane stress response in both *C. albicans* and *S. cerevisiae*, which activates the Pkc1 signaling pathway.

The chemical-genetic profile for clofazimine suggested it could be generating reactive oxygen species leading to an oxidative stress against *S. cerevisiae*. Similar mechanisms have been reported in *Mycobacterium smegmatus* such that growth of the bacteria in the presence of antioxidants blocks the toxic effects induced by clofazimine (Yano et al., 2011). To address this possibility we sought to determine if we could abolish the synergy observed between clofazimine and caspofungin upon addition of antioxidants; however the synergy observed between compounds was maintained in the presence of structurally diverse antioxidants α-tocopherol or *N*-acetyl-L-cysteine (Figure S5C). Thus, we propose that the primary mode of action of clofazimine in yeast is through membrane perturbation, not through the generation of oxidative stress.

Clofazimine potentiates antifungals in diverse fungal pathogens

To assess the clinical relevance of clofazimine as a combination agent against fungal pathogens we assessed its ability to potentiate caspofungin against diverse *Candida* species. MIC assays were performed using a gradient of caspofungin without and with a fixed dose of clofazimine. The addition of clofazimine reduced the caspofungin MIC for all *Candida* species tested (Figure 7A). Clofazimine also reduced the caspofungin MIC for three clinical isolates of *C. albicans* although to a lesser extent (Figure 7A). Next, we assessed whether clofazimine could be used as a combination agent to treat *A. fumigatus* infections, a leading fungal pathogen of humans. Checkerboard assays were performed with a gradient of caspofungin and clofazimine and growth was monitored by both optical density and by microscopy due to the filamentous nature of the fungus. Clofazimine potentiated the activity

of caspofungin against *A. fumigatus*, (Figure 7B) and dramatic reductions in *A. fumigatus* hyphal growth and alterations in hyphal morphology were observed with the drug combination relative to individual drug treatments (Figure 7C). Similar effects were seen with the azole posaconazole in combination with clofazimine (Figure 7C). Clofazimine thus enhances the efficacy of the azole and echinocandin antifungal classes in *A. fumigatus*.

We explored the therapeutic potential of clofazimine in combination with caspofungin against *C. albicans* in an *in vivo* model of infection. We used a tractable invertebrate model, the greater wax moth *G. mellonella*, to study candidiasis *in vivo*. We injected each larvae with 10^5 cells of a clinical isolate of *C. albicans* and monitored survival every 24-hours. Injection of larvae with *C. albicans* caused ~60% death within one day and 100% death after 4 days (Figure 7D). Treatment of injected larvae with low doses of individual drug treatments had no effect on survival. Strikingly, a combination treatment rescued growth of *G. mellonella* to a similar level as that observed in the vehicle control ($P < 0.001$, Log-rank test). Thus, combination therapy with clofazimine and caspofungin rescues lethal *C. albicans* infections in an *in vivo* invertebrate model.

DISCUSSION

There is an urgent unmet clinical need to identify new leads to treat systemic fungal infections. To address this need, we optimized a systematic approach to uncover compounds previously unknown to synergize with antifungal agents by combining sub-lethal concentrations of six known antifungals with ~3600 bioactive compounds, including hundreds of off-patent drugs. By exploring these interactions in evolutionary diverse fungal species we unveiled a broad spectrum of chemical-chemical interactions, which we termed the ACM. This dramatically expands the spectrum of previously known antifungal potentiators using molecules that are not employed as antifungals *per se*, but are small molecules previously approved for other indications with well-characterized pharmacokinetic properties or with other bioactivities. Within this rich dataset we identified a subset of drug combinations that were active against a fluconazole-resistant *C. albicans* clinical isolate, suggesting additional drug combinations in the ACM are likely active against drug-resistant fungal species. Finally, we determined the mechanism of action of clofazimine, an antimycobacterial compound for which antifungal activity had not previously been described, but which we showed has broad therapeutic potential against fungi. Thus, the ACM dataset is an invaluable resource for research and clinical communities to investigate combination therapeutics with favorable efficacy against harmful fungal pathogens.

Few antifungal potentiators are conserved across the different fungal species investigated in the ACM. Little cross species overlap was also observed in a previous study that specifically looked for potentiators of fluconazole (Spitzer et al., 2011). The highly specific effects drug combinations have on distinct species can be attributed to multiple factors. Hundreds of millions of years of evolution have altered the way different species respond to stress induced by small molecules. Fluconazole alone elicits distinct responses to cope with the drug-induced stress in different fungal species. *S. cerevisiae* enhances sterol import and *C. glabrata* enhances fluconazole export to tolerate azole exposure (Kuo et al., 2010). Further,

in *S. cerevisiae* and *C. albicans* distinct cellular circuitries involving the Pkc1 and calcineurin signal transduction cascades are involved in response to fluconazole (LaFayette et al., 2010). Recently, a large-scale chemogenomic atlas was generated for *C. neoformans* and was compared to similar chemical-genetic profiles in *S. cerevisiae* (Brown et al., 2014). The chemical-genetic interactions identified between fungal pathogen and model yeast were largely distinct, even among orthologous genes (Brown et al., 2014). Our work further reinforces the importance of pathogen-focused investigation and is the first dataset of this magnitude that explores combinatorial agents in two evolutionary diverse fungal pathogens.

A key public health concern is the rapid development of resistance many fungal pathogens, most notably *C. albicans*, have to current antifungal treatments (CDC, 2013). In a fluconazole resistant isolate of *C. albicans*, we observed potent synergistic interactions between fluconazole and chlorhexidine, hypocrellin A, or tomatidine. There are numerous mutations readily acquired in clinical settings that confer fluconazole resistance in *C. albicans* including, but not limited to, mutations in the azole target Erg11 and mutations involving upregulation of drug efflux pumps (Shapiro et al., 2011). The nature of the resistance mechanism often dictates whether particular drug combinations will be efficacious. Mutations in *TAC1*, a transcriptional activator of the *CDR* drug efflux pumps, maintain resistance to fluconazole in the presence of calcineurin or Hsp90 inhibitors (Hill et al., 2015). The clinical isolate used in our studies harbored several nonsynonymous substitutions in *TAC1*, including a hyperactive mutation, $Tac1^{T225A}$, capable of conferring fluconazole resistance (Coste et al., 2007). We also identified a nonsynonymous mutation in *ERG11* located in a `hot-spot' region predisposed to mutations that confer fluconazole resistance (Marichal et al., 1999). Although additional work remains to assess the impact each of these mutations has in conferring fluconazole resistance, it remains intriguing that chlorhexidine, hypocrellin A, and tomatidine are able to potentiate fluconazole in this strain and warrants further investigation into the manner by which they do so.

We selected clofazimine for mechanistic studies due to its broad, yet unreported, activity against diverse fungal species. A genome-wide chemical-genetic profile combined with cell biological phenotypes suggests clofazimine diffuses across the plasma membrane and intercalates into the cytosolic side of the lipid bilayer, which manifests in a cell membrane stress. This is supported by studies in bacteria that have shown clofazimine is a membrane-destabilizing agent, dismantling membrane architecture directly and by interacting with lysophospholipids (Cholo et al., 2012). Recently, derivatives of amphotericin B were generated that displayed high selectivity to pathogen-specific lipids *in vitro* and potent efficacy in mouse models of fungal pathogenesis (Davis et al., 2015). These compounds strongly evaded the emergence of resistance, likely because ergosterol serves as a central molecular node in a myriad of essential cellular processes (Davis et al., 2015). As our work implicates membrane lipids as a target of clofazimine, we postulate this compound could similarly impede resistance development. Clofazimine dramatically improved the efficacy of caspofungin in non-*albicans Candida*. Notably, the incidence of candidemia due to other *Candida* species such as *C. parapsilosis* and *C. glabrata* has increased significantly over the last two decades (Cleveland et al., 2012). Alarmingly, resistance to fluconazole and echinocandins is more common in non-*albicans Candida* compared with *C. albicans* isolates

(Cleveland et al., 2012), necessitating the development of new treatment strategies in these species. As predicted by our *in vitro* data, combination therapy with clofazimine and caspofungin rescues a lethal *C. albicans* infection in the invertebrate host *G. mellonella*. However, preliminary experiments in a mouse model of disseminated *C. albicans* infection did not support our *in vitro* data (Figure S6), presumably due to unfavourable pharmacokinetic properties against the drug combinations in this more complex model system. Additional experiments using altered routes of administration and/or infections with other fungal pathogens may still unveil conditions for the use of clofazimine as a treatment for fungal infections.

The generation of the ACM charted a new realm of chemical space, which has and will continue to be exploited for both fundamental biological research and as an approach to accelerate drug development. We know more efficacious and specific intervention for the treatment of infectious disease can be achieved through the combinations of bioactive compounds. The challenge that remains for us and other members of the medical mycology community is to identify and explore those combinations whose strong *in vitro* synergistic interactions can be translated to potent therapies in mammalian models of fungal infections.

EXPERIMENTAL PROCEDURES

Strains and Culture Conditions

Strains are listed in Table S7 and culture conditions are described in the Extended Experimental Procedures.

High-Throughput Screening

The McMaster Bioactives collection was screened at a final concentration of 12.5 μM in the presence and absence of ¼ MIC antifungal. Screens were performed using *C. albicans* (ATCC 90028), *C. neoformans* (H99), *S. cerevisiae* (BY4741), and *S. pombe* (ATCC 38366). Details of screening methods are described in the Extended Experimental Procedures. In brief, screens were conducted in duplicate in 384-well flat bottom microtitre plates (ThermoScientific) at a final volume of 80 μL. For preparation of diluted yeast culture, liquid overnight cultures were diluted to an OD_{600} of 0.14, followed by a 1:1000 dilution in SC media. Plates were incubated at 30°C and OD_{600} was measured after 48 h of growth for *S. cerevisiae* and *C. albicans* or 72 h of growth for *C. neoformans* and *S. pombe*. All data was normalized for plate- and row/column-specific effects as described previously (Spitzer et al., 2011). Screen hits were those compounds that were 3 MADs below the diagonal, inhibited growth on their own less than 50%, and resulted in at least 80% growth inhibition in the presence of the antifungal. Chemical-chemical interactions were generated using the program Cytoscape v3.2.1 using a spring embedded algorithm (http://www.cytoscape.org).

Drug Susceptibility Assays

All compounds were purchased from Sigma Aldrich with the exception for caspofungin (®Cancidas) and posaconazole, which were purchased from Merck Inc, and hypocrellin A, which was purchased from Abcam. Dimethyl sulfoxide (DMSO, Sigma Aldrich Co.) was

the solvent for all compounds. Drug susceptibility assays were performed as described previously (LaFayette et al., 2010). Details of protocol are described in the Extended Experimental Procedures. For *A. fumigatus*, drug susceptibility was determined using a 24-well plate assay (Corning, Inc.). Each well was inoculated with 10^5 conidia of *A. fumigatus* Af293. The plates were incubated at 37°C and 5% CO_2 and examined after 24 h and 48 h under an inverted light microscope (Zeiss, Inc.). Images acquired using Infinity2 camera (Lumenera, Inc.).

Cidality Assays

Viability of cultures after treatment with a gradient of fluconazole in combination with a gradient of ACM compound were tested by spotting 2 μL on YPD plates after yeast cells had been incubated with compound for 48 h. YPD agar plates were incubated at 30°C for 48 h prior to imaging.

Spotting Assays

Strains were grown to saturation in YPD and cell concentrations were standardized based on optical density. Fivefold dilutions (from ≈1×10^6 cells/ml) were spotted onto pH buffered media with and without clofazimine. Plates were photographed after 2 days in the dark at 30°C.

Chemical-Genomic Assays

S. cerevisiae deletion collections (*MAT***a** haploid and heterozygous essential deletion strains) were obtained from Research Genetics (Germany). Details of protocol are described in the Extended Experimental Procedures. In brief, compounds were screened at a concentration that inhibited growth of the pool by ~20% relative to a solvent control. Deletion pools were grown for 24 h and which point gDNA was extracted using phenol-chloroform extraction methods. Purified gDNA was used to amplify the barcoded tags upstream of the KANMX cassette using various primer combinations (Table S8). PCR products were pooled and sequenced at the Farncombe Metagenomics Facility at McMaster University. *P*-values for Gene Ontology (GO) enrichment were calculated through the Gene Ontology Consortium resource (http://geneontology.org) (Gene Ontology, 2015).

Immune Blot Analysis

Immunoblotting was conducted as described previously (LaFayette et al., 2010). In brief, a strain of *S. cerevisiae* harbouring a GFP epitope tag on Slt2 was grown overnight in YPD at 30°C without and with 10 μg/mL of clofazimine. In the morning, cells were diluted to OD_{600} of 0.2 in 125 mL of YPD without or with clofazimine, and grown to mid-log (~5 hours) at 30°C. Cultures were split and left untreated or treated with 50 ng/mL of caspofungin for 30 min. Cells were harvested and total protein extracts were prepared as described previously (Robbins et al., 2011). Protein concentrations were determined by Bradford analysis. Samples were separated by 10% SDS-PAGE. Protein was electrotransferred to PVDF membrane, blocked with 5% bovine serum albumin in tris buffered saline with 0.1% tween. Blots were hybridized with antibodies against GFP (1:750

dilution, Cell Signaling, 2956P) and phospho-p44/42 MAPK (Thr202/Tyr204) (1:750, Cell Signaling, 9101S).

G. mellonella Antifungal Assay

Injection of *C. albicans* and antifungal drugs was performed essentially as described (Fuchs et al., 2010). In brief, larvae in the final instar were obtained from Reptilia: Reptile Zoo and Educational Facility. Sixteen larvae (275 ± 25 mg) were used per group. Each injection of 5 μl of fungus, drug, or control into the hemocoel was performed via a distinct proleg. Drugs were injected after inoculum delivery. Larvae were incubated at 37°C and the number of dead larvae scored daily. *C. albicans* inoculum was prepared by growing YPD cultures overnight at 30 °C. Cells washed 3 times in PBS, densities were determined by hemacytometer count and dilutions prepared in PBS. Kill curves were plotted and estimation of differences in survival (Log-rank test) analyzed by the Kaplan-Meier method (GraphPad Prism). Killing assays were performed twice using distinct batches of *G. mellonella*.

Supplementary Material

Refer to Web version on PubMed Central for supplementary material.

ACKNOWLEDGEMENTS

We thank Leah Cowen for strains; and Leah Cowen, Troy Ketela, and Wright lab members for helpful discussions. NR was supported by the Michael G. DeGroote Postdoctoral Fellowship Award and a Canadian Institute for Health Research (CIHR) Fellowship. GDW and MT were supported by Canada Research Chairs in Antibiotic Biochemistry and Systems and Synthetic Biology respectively. Research was funded by grants from CIHR (MOP 119572 to MT and GDW), the European Research Council (SCG-233457 to MT), the National Institutes of Health (1R01-AI112595 to JH) and the Wellcome Trust (085178 to MT).

REFERENCES

Anderson N, Borlak J. Drug-induced phospholipidosis. FEBS letters. 2006; 580:5533–5540. [PubMed: 16979167]

Anderson TM, Clay MC, Cioffi AG, Diaz KA, Hisao GS, Tuttle MD, Nieuwkoop AJ, Comellas G, Maryum N, Wang S, et al. Amphotericin forms an extramembranous and fungicidal sterol sponge. Nat Chem Biol. 2014; 10:400–406. [PubMed: 24681535]

Blankenship JR, Steinbach WJ, Perfect JR, Heitman J. Teaching old drugs new tricks: reincarnating immunosuppressants as antifungal drugs. Curr Opin Investig Drugs. 2003; 4:192–199.

Borisy AA, Elliott PJ, Hurst NW, Lee MS, Lehar J, Price ER, Serbedzija G, Zimmermann GR, Foley MA, Stockwell BR, et al. Systematic discovery of multicomponent therapeutics. Proc Natl Acad Sci USA. 2003; 100:7977–7982. [PubMed: 12799470]

Brown GD, Denning DW, Gow NA, Levitz SM, Netea MG, White TC. Hidden killers: human fungal infections. Science Transl Med. 2012; 4:165rv113.

Brown JC, Nelson J, VanderSluis B, Deshpande R, Butts A, Kagan S, Polacheck I, Krysan DJ, Myers CL, Madhani HD. Unraveling the biology of a fungal meningitis pathogen using chemical genetics. Cell. 2014; 159:1168–1187. [PubMed: 25416953]

Butts A, DiDone L, Koselny K, Baxter BK, Chabrier-Rosello Y, Wellington M, Krysan DJ. A repurposing approach identifies off-patent drugs with fungicidal cryptococcal activity, a common structural chemotype, and pharmacological properties relevant to the treatment of cryptococcosis. Eukaryot Cell. 2013; 12:278–287. [PubMed: 23243064]

Centers for Disease Control and Prevention. U.S. Department of Health and Human Services. CDC; Atlanta, GA: 2013. Antibiotic Resistance Threats in the United States, 2013.

Cholo MC, Steel HC, Fourie PB, Germishuizen WA, Anderson R. Clofazimine: current status and future prospects. Journal Antimicrob Chemother. 2012; 67:290–298. [PubMed: 22020137]

Cleveland AA, Farley MM, Harrison LH, Stein B, Hollick R, Lockhart SR, Magill SS, Derado G, Park BJ, Chiller TM. Changes in incidence and antifungal drug resistance in candidemia: results from population-based laboratory surveillance in Atlanta and Baltimore, 2008–2011. Clinical infectious diseases : an official publication of the Infectious Diseases Society of America. 2012; 55:1352–1361. [PubMed: 22893576]

Costanzo M, Baryshnikova A, Bellay J, Kim Y, Spear ED, Sevier CS, Ding H, Koh JL, Toufighi K, Mostafavi S, et al. The genetic landscape of a cell. Science. 2010; 327:425–431. [PubMed: 20093466]

Coste A, Selmecki A, Forche A, Diogo D, Bougnoux ME, d'Enfert C, Berman J, Sanglard D. Genotypic evolution of azole resistance mechanisms in sequential *Candida albicans* isolates. Eukaryot Cell. 2007; 6:889–904. [PubMed: 17468392]

Cowen LE, Singh SD, Kohler JR, Collins C, Zaas AK, Schell WA, Aziz H, Mylonakis E, Perfect JR, Whitesell L, et al. Harnessing Hsp90 function as a powerful, broadly effective therapeutic strategy for fungal infectious disease. Proc Natl Acad Sci USA. 2009; 106:2818–2823. [PubMed: 19196973]

Davis SA, Vincent BM, Endo MM, Whitesell L, Marchillo K, Andes DR, Lindquist S, Burke MD. Nontoxic antimicrobials that evade drug resistance. Nat Chem Biol. 2015; 11:481–7. [PubMed: 26030729]

Day JN, Chau TT, Wolbers M, Mai PP, Dung NT, Mai NH, Phu NH, Nghia HD, Phong ND, Thai CQ, et al. Combination antifungal therapy for cryptococcal meningitis. N Engl J Med. 2013; 368:1291–1302. [PubMed: 23550668]

De Filippi L, Fournier M, Cameroni E, Linder P, De Virgilio C, Foti M, Deloche O. Membrane stress is coupled to a rapid translational control of gene expression in chlorpromazine-treated cells. Curr Genet. 2007; 52:171–185. [PubMed: 17710403]

Denning DW, Bromley MJ. Infectious Disease. How to bolster the antifungal pipeline. Science. 2015; 347:1414–1416. [PubMed: 25814567]

Fuchs BB, O'Brien E, Khoury JB, Mylonakis E. Methods for using *Galleria mellonella* as a model host to study fungal pathogenesis. Virulence. 2010; 1:475–482. [PubMed: 21178491]

Gene Ontology C. Gene Ontology Consortium: going forward. Nucleic acids research. 2015; 43:D1049–1056. [PubMed: 25428369]

Giaever G, Flaherty P, Kumm J, Proctor M, Nislow C, Jaramillo DF, Chu AM, Jordan MI, Arkin AP, Davis RW. Chemogenomic profiling: identifying the functional interactions of small molecules in yeast. Proc Natl Acad Sci USA. 2004; 101:793–798. [PubMed: 14718668]

Gilbert P, Moore LE. Cationic antiseptics: diversity of action under a common epithet. J Appl Microbiol. 2005; 99:703–715. [PubMed: 16162221]

Hill JA, O'Meara TR, Cowen LE. Fitness Trade-Offs Associated with the Evolution of Resistance to Antifungal Drug Combinations. Cell Reports. 2015; 10:809–819.

Kuo D, Tan K, Zinman G, Ravasi T, Bar-Joseph Z, Ideker T. Evolutionary divergence in the fungal response to fluconazole revealed by soft clustering. Genome Biol. 2010; 11:R77. [PubMed: 20653936]

LaFayette SL, Collins C, Zaas AK, Schell WA, Betancourt-Quiroz M, Gunatilaka AA, Perfect JR, Cowen LE. PKC signaling regulates drug resistance of the fungal pathogen *Candida albicans* via circuitry comprised of Mkc1, calcineurin, and Hsp90. PLoS Pathog. 2010; 6:e1001069. [PubMed: 20865172]

Lee AY, St Onge RP, Proctor MJ, Wallace IM, Nile AH, Spagnuolo PA, Jitkova Y, Gronda M, Wu Y, Kim MK, et al. Mapping the cellular response to small molecules using chemogenomic fitness signatures. Science. 2014; 344:208–211. [PubMed: 24723613]

Levin DE. Cell wall integrity signaling in *Saccharomyces cerevisiae*. Microbiol Mol Biol Rev. 2005; 69:262–291. [PubMed: 15944456]

Marichal P, Koymans L, Willemsens S, Bellens D, Verhasselt P, Luyten W, Borgers M, Ramaekers FC, Odds FC, Bossche HV. Contribution of mutations in the cytochrome P450 14alpha-

demethylase (Erg11p, Cyp51p) to azole resistance in *Candida albicans*. Microbiology. 1999; 145:2701–2713. [PubMed: 10537192]

Odds FC. Synergy, antagonism, and what the chequerboard puts between them. J Antimicrob Chemother. 2003; 52:1. [PubMed: 12805255]

Ostrosky-Zeichner L, Casadevall A, Galgiani JN, Odds FC, Rex JH. An insight into the antifungal pipeline: selected new molecules and beyond. Nat Rev Drug Disc. 2010; 9:719–727.

Pierce SE, Fung EL, Jaramillo DF, Chu AM, Davis RW, Nislow C, Giaever G. A unique and universal molecular barcode array. Nat Methods. 2006; 3:601–603. [PubMed: 16862133]

Robbins N, Uppuluri P, Nett J, Rajendran R, Ramage G, Lopez-Ribot JL, Andes D, Cowen LE. Hsp90 governs dispersion and drug resistance of fungal biofilms. PLoS Pathog. 2011; 7:e1002257. [PubMed: 21931556]

Shapiro RS, Robbins N, Cowen LE. Regulatory circuitry governing fungal development, drug resistance, and disease. Microbiol Mol Biol Rev. 2011; 75:213–267. [PubMed: 21646428]

Sharom JR, Bellows DS, Tyers M. From large networks to small molecules. Curr Opin Chem Biol. 2004; 8:81–90. [PubMed: 15036161]

Simons V, Morrissey JP, Latijnhouwers M, Csukai M, Cleaver A, Yarrow C, Osbourn A. Dual effects of plant steroidal alkaloids on *Saccharomyces cerevisiae*. Antimicrob Agent Chemother. 2006; 50:2732–2740.

Spitzer M, Griffiths E, Blakely KM, Wildenhain J, Ejim L, Rossi L, De Pascale G, Curak J, Brown E, Tyers M, et al. Cross-species discovery of syncretic drug combinations that potentiate the antifungal fluconazole. Mol Systems Biol. 2011; 7:499.

Wilson LS, Reyes CM, Stolpman M, Speckman J, Allen K, Beney J. The direct cost and incidence of systemic fungal infections. Value Health. 2002; 5:26–34. [PubMed: 11873380]

Yano T, Kassovska-Bratinova S, Teh JS, Winkler J, Sullivan K, Isaacs A, Schechter NM, Rubin H. Reduction of clofazimine by mycobacterial type 2 NADH:quinone oxidoreductase: a pathway for the generation of bactericidal levels of reactive oxygen species. J Biol Chem. 2011; 286:10276–10287. [PubMed: 21193400]

Zimmermann GR, Lehar J, Keith CT. Multi-target therapeutics: when the whole is greater than the sum of the parts. Drug Disc Today. 2007; 12:34–42.

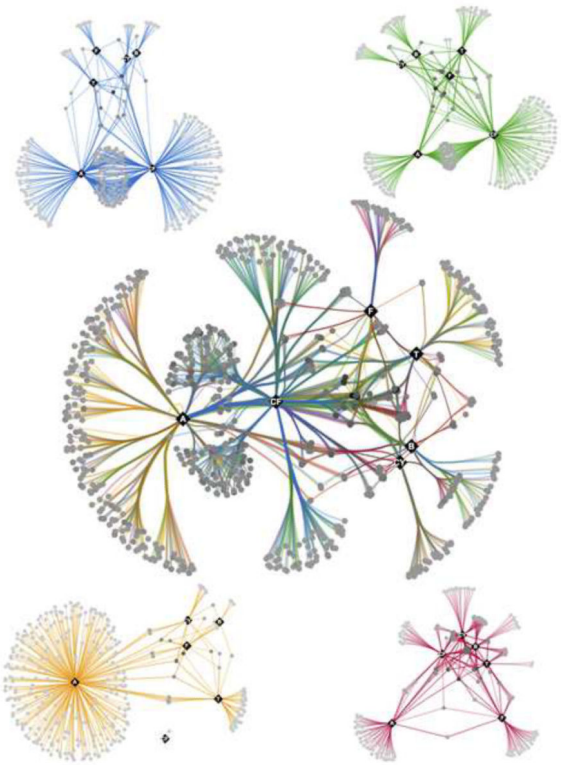

Figure 1. The ACM chemical-chemical interaction network

The central chemical-chemical interaction network comprises a total of 1550 chemical interactions. Compounds that potentiated an antifungal are depicted as circles and are connected by edges to the antifungal in which synergy is observed. Edges are colored to represent interactions identified against different fungal species with blue representing *C. albicans*, green representing *S. cerevisiae*, orange representing *C. neoformans*, and red representing *S. pombe*. Antifungals are shown as black diamonds. (Amphotericin B (A), benomyl (B), caspofungin (CF), cyprodinil (CY), fluconazole (F) or terbinafine (T)). Chemical-chemical networks for each individual species are plotted in corners and are colored as described above. See also Figure S1, Figure S2, Table S1, Table S2, and Table S3.

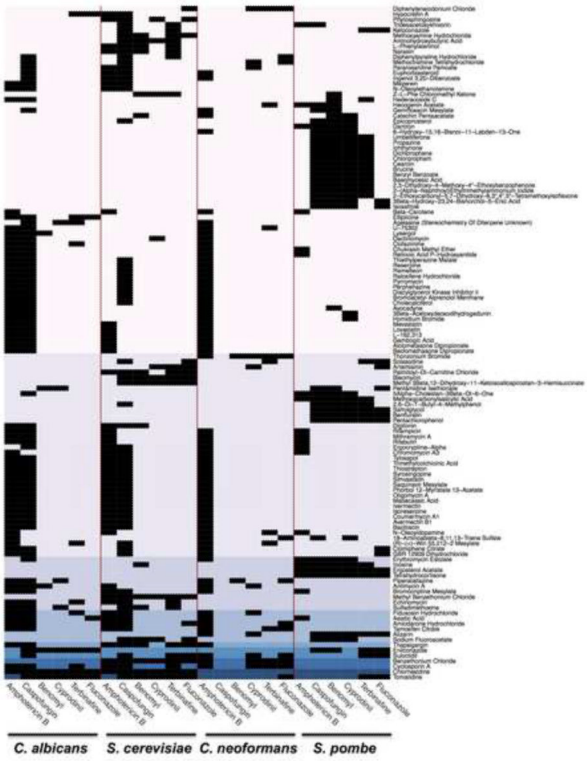

Figure 2. High-connectivity compounds from the ACM

Those compounds that were identified in 4 or more screens were visualized on a heat map. Black rectangles represent conditions where molecules potentiated the antifungal. Background color represents the number of screens in which a molecule was identified with dark blue representing 12 or more screens and light pink representing four screens. The names of compounds that potentiated antifungals are listed on the right and screening conditions are highlighted at the bottom. The heat map is organized by species and similarity of screening hits. See also Figure S1, Figure S2, Table S2 and Table S3.

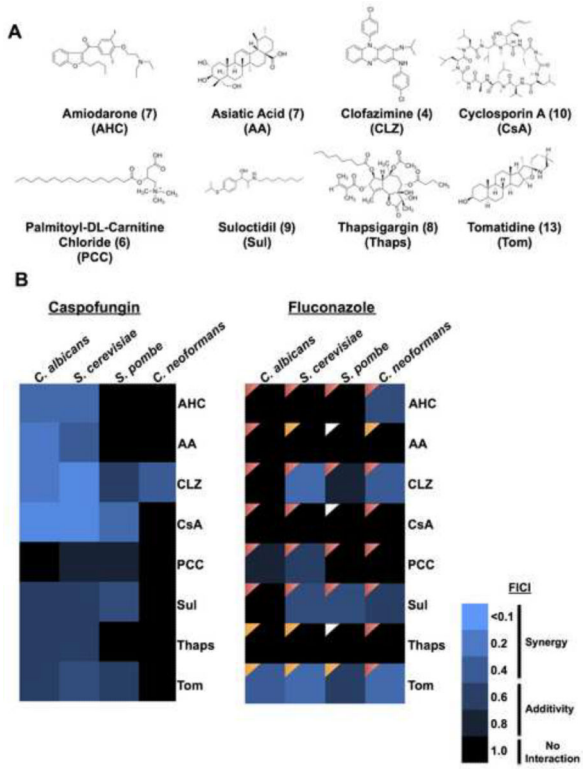

Figure 3. ACM hit validation and characterization

A) Structures of compounds identified as potentiators in the ACM. The numbers shown in brackets indicate the number of screens in which they were identified. See also Table S4. **B)** Heat map of drug interactions with caspofungin or fluconazole in each species as measured by fractional inhibition concentration index (FICI). Light blue indicates synergistic drug interactions (FICI < 0.5); darker shades of blue represent additivity (FICI 0.5–0.99); black represents no interaction (FICI 1.0–4.0). Compounds tested in combination with fluconazole were examined for cidality. Red triangles indicate a fungicidal drug combination, orange triangles indicate fungistatic drug combinations and white triangles indicate conditions where no inhibition of growth was observed mitigating cidality testing. See also Figure S3, Table S4 and Table S5.

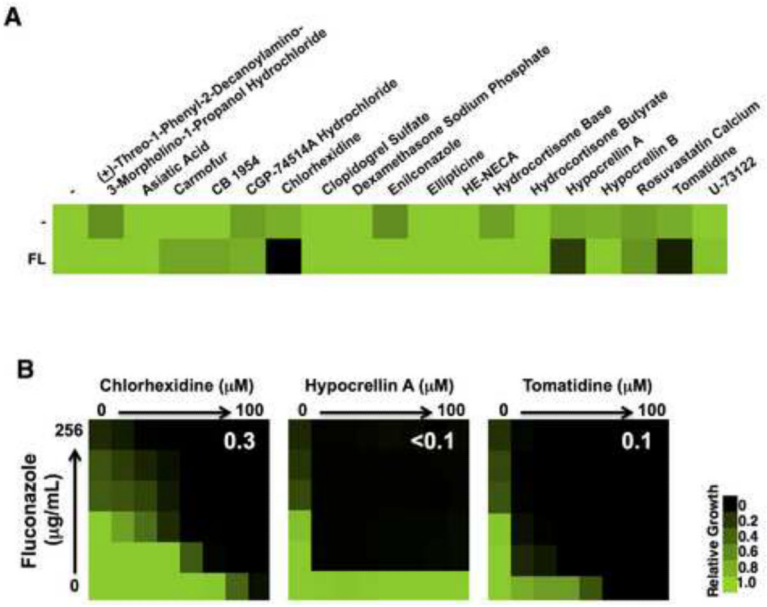

Figure 4. Drug combinations with efficacy against a clinically resistant isolate of *C. albicans*

A) The 18 compounds identified as potentiators of fluconazole (FL) against *C. albicans* in the ACM were tested against a fluconazole resistant clinical isolate. *C. albicans* was grown in the absence (−) or presence of ¼ MIC (32 μg/mL) of FL in combination with the ACM hits (12.5 μM). Growth was measured by OD_{600} and data was quantitatively displayed with color using Treeview (see color bar). **B)** Checkerboard assays highlight drug interactions between fluconazole with chlorhexidine, hypocrellin A, or tomatidine. Growth was monitored and analyzed as described in part A. White numbers indicate calculated FICI values.

A

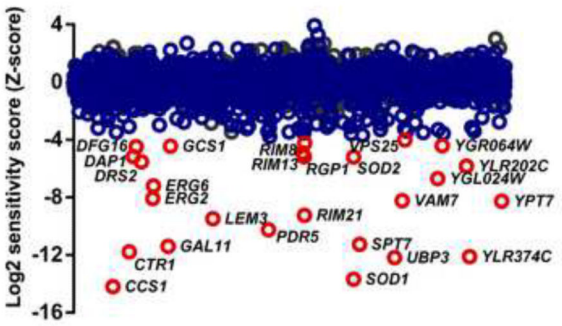

B

GO Biological Process Complete	No. Genes Identified in Each Catergory	No. Genes Expected in Each Category	Fold Enrichment	*P*-value
phospholipid transport	5	0.3	>5	2.54E-02
ubiquitin-dependent protein catabolic process via the MVB sorting pathway	5	0.31	>5	3.17E-02
single-organism membrane organization	15	3.89	3.86	1.34E-02
membrane organization	15	3.95	3.8	1.59E-02
vesicle-mediated transport	18	5.12	3.52	5.20E-03
negative regulation of cellular metabolic process	18	5.94	3.03	3.99E-02
cellular localization	29	12.62	2.3	1.75E-02
single-organism transport	32	15.08	2.12	2.61E-02
transport	37	17.65	2.1	5.04E-03
single-organism localization	34	16.39	2.07	2.01E-02
localization	41	20.05	2.05	1.89E-03
establishment of localization	37	18.22	2.03	1.09E-02
regulation of biological process	42	22.27	1.89	1.15E-02
regulation of cellular process	40	21.4	1.87	2.86E-02
biological regulation	47	25.35	1.85	3.08E-03
single-organism cellular process	67	46.49	1.44	2.58E-02
unclassified	8	10	0.8	0.00E+00

Figure 5. Genome-wide chemical-genetic interactions for clofazimine

A) Sensitivity of heterozygous essential deletion strains (gray circles) and homozygous deletion strains (blue circles) to clofazimine as assessed by HIP and HOP. Data represents the average Z score for two biological replicates. Those haploid deletion strains that have a Z-score more significant than three standard-deviations below the mean are highlighted in red. No heterozygous deletion strains were identified with a Z-score less than three standard-deviations below the mean. See also Table S6. **B)** Gene Ontology (GO) Biological Process terms were generated for those deletion mutants that were at least two standard deviations more sensitive to clofazimine than the mean population. *P* values were calculated using PANTHER Overrepresentation Test via GO Ontology Database. See also Figure S4.

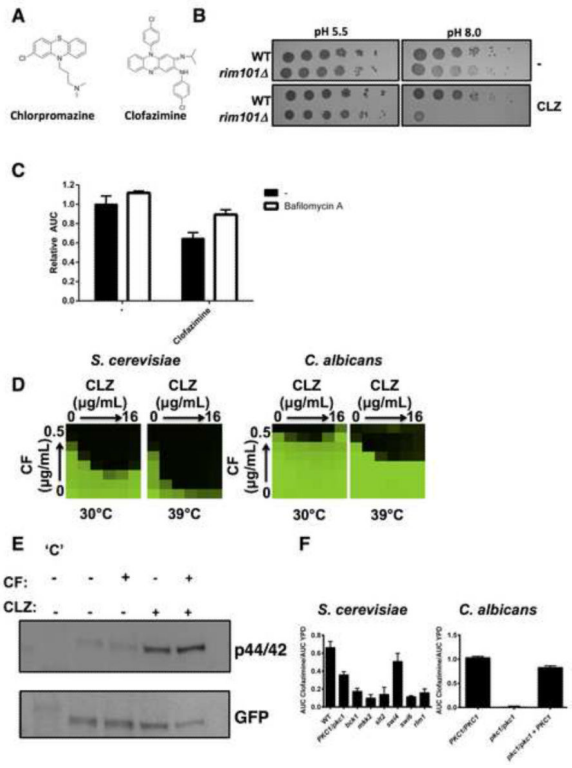

Figure 6. Clofazimine acts as a membrane perturbing agent in fungi

A) Structures of the membrane perturbing agent chlorpromazine and clofazimine. **B)** Acidic pH blocks the toxic effects observed by clofazimine (CLZ). Cells were spotted in fivefold dilutions from ~1×10^6 cells/mL onto solid buffered YPD medium with 32 μg/mL of clofazimine as indicated. **C)** Clofazimine-induced toxicity is rescued by bafilomycin A. Growth of *S. cerevisiae* was monitored by measuring the OD_{600} for 36 hours. Area under the curve (AUC) was calculated and normalized to solvent treated control. Data are means ± standard deviation of triplicate experiments. **D)** Elevated temperature exacerbates the synergy observed between CF and CLZ. Checkerboards were performed and analyzed as in Figure 4. **E)** Treatment of *S. cerevisiae* with CLZ activates Pkc1 signaling as measured by Slt2 phosphorylation. A strain of *S. cerevisiae* harbouring an allele of *SLT2* C-terminally GFP tagged was treated with CLZ or CF as indicated. Total protein was resolved by SDS-PAGE and blots were hybridized with an α-phospho p44/42 MAPK antibody to monitor phosphorylated Slt2 levels and an α-GFP antibody to monitor total Slt2 levels. `C' indicates untagged control strain. **F)** Deletion mutants in *S. cerevisiae* or *C. albicans* were grown in the absence and presence of 128 μg/mL CLZ for 26 hours. Area under the curve (AUC) was calculated in the presence and absence of drug. Data are means ± standard deviation of quadruplicates. See also Figure S5.

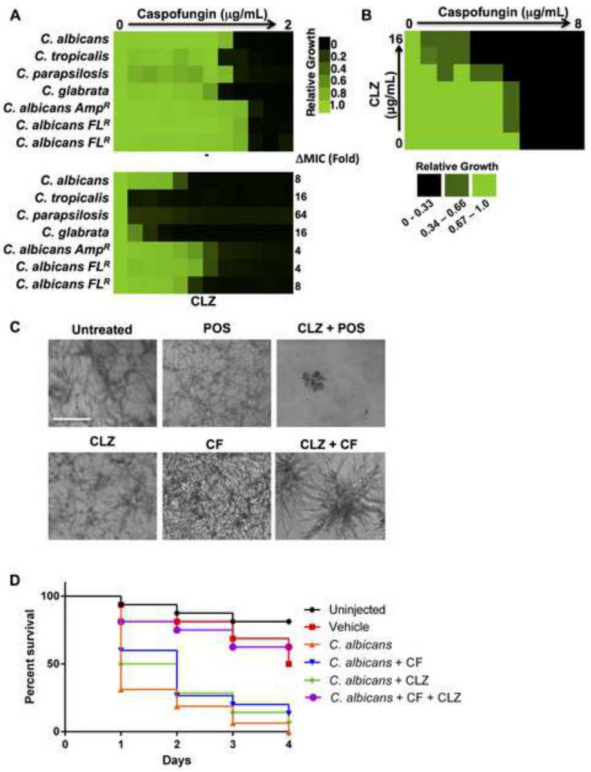

Figure 7. Clofazimine potentiates antifungals in evolutionary diverse fungal pathogens and in an in vivo model of infection

A) Caspofungin (CF) MIC assays were conducted against multiple non *albicans Candida* species and against clinical isolates of *C. albicans* that are known to be resistant to indicated antifungals. MICs were conducted in the absence (−) or presence of a fixed concentration of clofazimine (CLZ). Changes in MIC in the presence of CLZ are indicated. Data was analyzed as described in Figure 4. **B)** Checkerboard analysis was conducted with a gradient of caspofungin and a gradient of CLZ in *A. fumigatus*. Growth was quantified and analyzed as described in Figure 4. See scale bar. **C)** Images show *A. fumigatus* incubated with CLZ (16 μg/mL) in combination with posaconazole (POS, 0.0625 μg/mL) or CF (0.125 μg/mL). Images were acquired at a 20× magnification. Scale bar represents 100 μM. **D)** CLZ potentiates CF in a *G. mellonella* host-model system. Sixteen larvae per treatment group were infected with 10^5 cells of a clinical isolate of *C. albicans*. Larvae were treated with CF (0.01 mg/kg), CLZ (15 mg/kg), or a combination once following infection and were scored daily for viability. *P* values generated by Log-Rank (Mantel-Cox) test. See also Figure S6.